2014 IEEE International Conference on Robotics & Automation (ICRA)
Hong Kong Convention and Exhibition Center
May 31 - June 7, 2014. Hong Kong, China

Slip Mitigation Control for an Electric Powered Wheelchair

Oscar Chuy*, Emmanuel G. Collins*, and Camilo Ordonez*
Jorge Candiotti**, Hongwu Wang**, and Rory Cooper**

***Abstract*— Most wheelchairs have low directional stability due to their wheel-drive system configurations. Hence, when a wheelchair experiences excessive slip, it will create an uncontrollable moment that changes its heading direction, endangering the safety of the wheelchair user. This paper presents an approach to longitudinal slip reduction (or traction control) for an Electric Powered Wheelchair that uses a variable reference model, which is a mass-damper system. The position of a joystick is mapped to force and torque values, which are the input to this model. The output is the desired trajectory, which is fed to a trajectory tracking controller. The key idea is that if slip occurs, the applied torque to the wheels is reduced by decreasing the desired acceleration, which is achieved by changing the parameters of the reference model. In this study, the mass of the reference model is changed. The proposed slip reduction approach is validated via experiments.**

I. Introduction

Electric Powered Wheelchairs (EPWs) are assistive devices that provide mobility for people who have suffered lower and possibly upper extremity impairments. They are heavily used in both indoor and outdoor environments and although the design of EPWs has greatly advanced over the years, the control systems have not significantly improved [2]. EPWs are typically driven by only two wheels and have caster wheels in the front and/or back. Hence, they are either mid-drive (caster wheels in the front and back), rear drive (caster wheels only in the front), or front drive (caster wheels only in the back) systems. Although caster wheels provide vertical stability, they do not increase lateral stability, and hence EPWs have inherently low lateral stability. It follows that a loss of traction in one of the wheels will significantly alter their heading direction as shown in Fig. 1, endangering the safety of the users.

A traction control approach was developed based on reducing the desired velocity when slip is detected [13]. The calculation of slip was based on an encoder attached to a caster wheel. Considering that a caster wheel is free to rotate about the vertical axis, the velocity of the caster must be projected along the direction of the drive wheels. This requires the use of an absolute position sensor to monitor the orientation of the castor. Based on our experience in implementing the approach in [13], it has problems in accurately estimating the actual slip, especially when the EPW traverses uneven terrain.

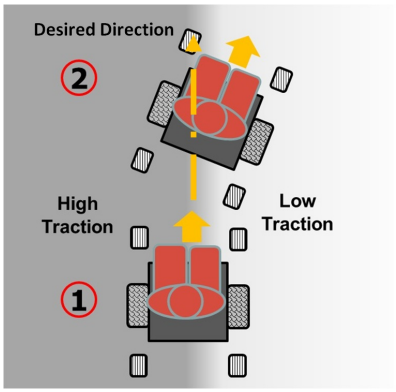

Fig. 1. An EPW is difficult to steer without slip mitigation control when one or more of the wheels moves on a slippery surface. Here, the user intent is to move straight along the longitudinal direction. However, due to loss of traction in the right drive wheel, the heading direction is significantly altered.

Model Following Control (MFC) is a traction control methodology for electric vehicles, including EPWs, [5], [6] and was introduced along with optimal slip control, which is discussed further in the next paragraph. In the MFC framework, the commanded torque $\tau_{d,i}$ to wheel i is input to the vehicle model, expressed about a coordinate axis centered at the corresponding wheel, to determine $\omega_{p,i}$, a prediction of the wheel angular velocity. The actual wheel velocity $\omega_{a,i}$ is measured and the controller torque $\tau_{c,i}$ is given by $\tau_{c,i} = K_{MFC,i}(\omega_{a,i} - \omega_{p,i})$, where $K_{MFC,i}$ is the MFC gain. The torque $\tau_i = \tau_{d,i} - \tau_{c,i}$ is then applied to wheel i. Note that as the wheel slips, $\omega_{a,i}$ increases, increasing

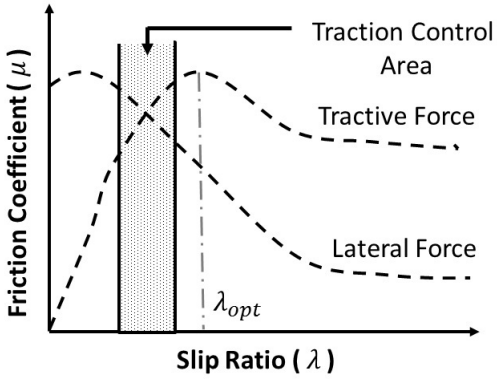

Fig. 2. The coefficient of friction varies with the slip ratio for both the tractive (longitudinal) force and the lateral force. As the slip ratio increases, the lateral force decreases, leading to loss of directional control or even instability [5].

*O. Chuy, E. G. Collins, and C. Ordonez are with the Center for Intelligent Systems, Control and Robotics (CISCOR) and the Department of Mechanical Engineering, Florida A&M University-Florida State University, Tallahassee, FL 32310, USA {chuy,ecollins,camilor}@eng.fsu.edu.

** J. Candiotti, H. Wang, and R. Cooper are with the Human Engineering Research Laboratory, University of Pittsburgh.

The funding for this research was provided by the National Science Foundation, Project EEC-0540865.

$\omega_{a,i} - \omega_{p,i}$ and thereby reducing τ_i. One limitation of MFC is that the MFC gain is dependent upon the terrain surface or road condition and a variations in this condition can severely change the performance of the traction control.

The desire to achieve a specific slip ratio led to several studies in slip control [3], [4], [6], [9], [11]. However, the more fundamental problem is to determine the optimal slip ratio. Based on Fig. 2, the slip ratio λ should be in $\{\lambda : 0 < \lambda \leq \lambda_{opt}\}$, where λ_{opt} is the slip ratio corresponding to μ_{max}, the maximum coefficient of friction corresponding to the tractive force . However, λ_{opt} varies with both the terrain type and surface conditions (e.g., degree of wetness). In [5], [6], [9], a proportional plus integral (PI) controller was used to drive λ to λ_{opt}, which was determined offline. The output torque of the PI controller was subtracted from the commanded torque and the actual slip ratio was determined by comparing the velocity of the driven wheels with the velocity of the non-driven wheels. The problems of the aforementioned slip control are as follows: 1) the methodology of determining the actual slip ratio is not applicable to all-wheel drive vehicles without redundant wheels, and 2) λ_{opt} must be determined online for practical implementation, which is difficult to achieve. Although online approaches to estimate λ_{opt} have been presented [10], [12], the estimates can be inaccurate due to sensor noise, especially since the approaches require differentiating noisy signals. The above limitations led to development of a traction control approach that does not depend on λ_{opt} [14], [15]. This method, called the Maximum Transferable Torque Estimate approach, is described in Sec. II.

Traction control approaches discussed in [5], [6], [14], [15] generally alter the commanded torque to the wheels when slip occurs. Hence, to develop traction control for an EPW, a control methodology that can directly or indirectly control the commanded torque and addresses human joystick interaction is needed. In [1], joystick positions are mapped into velocity and direction commands. For example in the longitudinal direction, the linear velocity is $v_x = k_x p_x$, where p_x is the joystick displacement and k_x is a proportionality constant. The acceleration and position components can then be determined respectively by differentiating and integrating the velocity v_x. Although the acceleration command plays a major part in the resulting command torque, this approach does not enable control of the acceleration since the model parameter k_x only directly effects the velocity component. Additionally, the resulting trajectory is not smooth since the sensor noise in p_x directly influences the commanded velocity. Hence, although this approach does map human intention to a commanded trajectory, it cannot be used to implement slip reduction.

Omni-directional motorized walkers have been controlled using mass-damper systems as reference models, one for each degree of freedom (x, y, θ) [7], [8], [16]. The human intentions, read by a force/torque sensor, are represented by the forces f_x and f_y and the torque n_z, which are fed to reference models to yield commanded trajectories for the robotic walkers. The parameters of the reference models are selected based on the physical constraints (e.g., maximum walking speed) of the user and also the constraints (e.g., maximum acceleration and velocity) of the robot system. For example, along the longitudinal direction, the reference model is $m_x\ddot{x} + d_x\dot{x} = f_x$. The parameter d_x is chosen to satisfy $d_x \geq f_{x_{max}}/v_{x_{max}}$, where $f_{x_{max}}$ represents the force corresponding to the maximum human input along the longitudinal direction and $v_{x_{max}}$ is the maximum desired velocity $\dot{x}$ along the longitudinal direction. The parameter m_x is chosen to satisfy $m_x \geq f_{x_{max}}/a_{max}$, where a_{max} is the maximum desired acceleration along the longitudinal direction.

The above reference model approach provides a viable structure to implement slip mitigation control since it can indirectly alter the commanded torque by modifying the mass parameter. Such an approach is developed here and unlike [7], [8], [16] is heavily dependent upon an estimate of the maximum tractive forces that can be applied to each wheel. These estimates are ultimately used to develop a lower bound on m_x that must be satisfied to avoid slip. Hence to mitigate slip, the control approach varies m_x, which is a novel concept in slip reduction.

In summary, the current slip and traction control methodologies are based on directly limiting the applied torque to the motors, which is highly applicable to open-loop systems where there is no trajectory tracking controller [5], [14], [15]. However, when feedback control is employed, directly limiting the applied torque can create substantial tracking errors, which accumulate over time. An approach which can be applied to EPWs is to indirectly alter the applied motor torque through the command trajectory when slip occurs. This can be achieved through modifying the desired reference model for EPWs so that the resulting command motor torque is within the limits that ensure little or no wheel slip.

II. Maximum Tractive Force Estimation

Assume that a vehicle has n wheels. In [14], [15] the vehicle model expressed about wheel i is considered, as shown in Fig. 3(a). The corresponding rotational dynamics are described by

$$J_{w,i}\dot{\omega}_{w,i} = \tau_i - \tau_{r,i} - rF_{d,i}, \tag{1}$$

where $J_{w,i}$ is the wheel inertia, $\dot{\omega}_{w,i}$ is the wheel angular acceleration, τ_i is the torque applied to the wheel, $\tau_{r,i}$ is the torque due to the gear resistance, r_i is the wheel radius and $F_{d,i}$ is the tractive force. The translational dynamics of the vehicle may be described in terms of wheel i by

$$M_i\dot{v}_i = F_{d,i} - F_{r,i}, \tag{2}$$

where v_i is the translational velocity of wheel i, M_i is the mass of the vehicle seen by wheel i, and $F_{r,i}$ is the resistance term (i.e., rolling resistance and drag) experienced at wheel i. Note that the total mass of the vehicle is given by $M = \sum_{i=1}^{n} M_i$ and the total resistance is given by $F_r = \sum_{i=1}^{n} F_{r,i}$. The Maximum Transferrable Torque Estimate (MTTE) approach [14], [15] requires solving for the maximum torque $\tau_{i,max}$ that achieves a desired value of

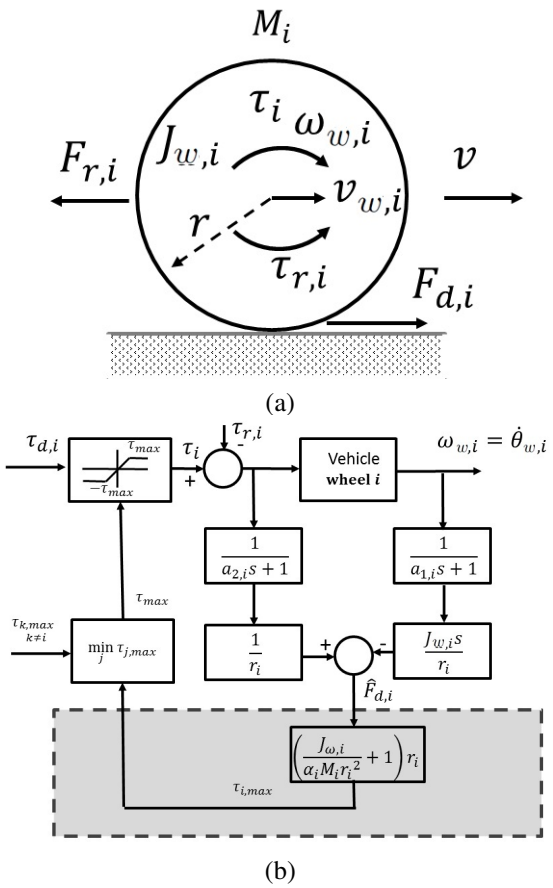

Fig. 3. (a) A key to the Maximum Transferable Torque Estimate (MTTE) approach to slip mitigation control is to express the vehicle dynamics about wheel i. (b) The MTTE approach can be implemented as shown in this diagram; the n wheels of the vehicle compute estimates $\hat{F}_{d,1}, \ldots, \hat{F}_{d,n}$ of the corresponding tractive forces and these estimates are used to limit the torques applied to each wheel so that no wheel requests a higher tractive force than can be applied to itself or any of the remaining wheels.

$\alpha_i > \dot{v}_i/\dot{v}_{w,i}$, which is the ratio of the actual translational acceleration to the estimate of the translational acceleration based on the wheel i angular acceleration. For the vehicle not to experience excessive slip, $\alpha_i < 1$ should satisfy $\alpha_i \approx 1$. Equations (1) and (2) can be solved for $\tau_{i,max}(= \tau_i)$, which under the assumptions $\tau_{r,i} = 0$ and $F_{r,i} << F_{d,i}$ yields $\tau_{i,max} = (J_{w,i}/(\alpha_i M_i r_i^2) + 1) r_i F_{d,i}$[15].

Fig. 3(b) shows how the tractive force $\hat{F}_{d,i}$ is estimated. It also shows that if the commanded torque $\tau_{d,i} > \tau_{max}$, where $\tau_{max} = \min_{j\in\{1,2,\ldots,n\}} \tau_{j,max}$, then $\tau_i = \tau_{max}$, otherwise $\tau_i = \tau_{d,i}$. In MTTE, τ_{max} is varied instead of directly altering τ_i as done in [6]. The results in [5], [14], [15] show that if slip occurs, the control approach shown in Fig. 3(b) is able to prevent further slip. However, in a control framework that uses a trajectory tracking controller, directly modifying the control torque τ_i causes undesirable trajectory errors, which grow over time. Hence, the proposed research aims to develop wheelchair commands that ensure that the wheel angular acceleration is modified such that for each wheel $\hat{F}_{d,i} < \hat{F}_{d_{max}} = \min_{j\in\{1,2,\ldots,n\}} \hat{F}_{d,j_{max}}$, where $\hat{F}_{d,j_{max}}$ is an estimate of the maximum tractive force for wheel j on the surface it is contacting.

Fig. 4. The experimental setup used in this study is a commercially available wheelchair electronically modified to handle real-time control. The computing system is mounted on the back of the chair.

III. Experimental Setup

Fig. 4 shows the EPW experimental platform that will be used in this study. It is a commercially available, differentially steered EPW, which is modified for real-time control. This EPW is propelled by two motors and has two front and back casters for balancing. The motors are driven by current-controlled motor drivers and they are equipped with encoders that are directly coupled to their shafts. A data acquisition board (i.e., a Sensoray 526) is used to read joystick signals and also processes the encoder signals. The board has several digital to analog channels used to send command signals to the motor drivers. A PIII-computer system controls the experimental setup and runs the QNX operating system such that the sampling rate is $1kHz$.

Fig. 5 shows the trajectory tracking controller used to control wheel i of the experimental setup. The inputs are the desired angular acceleration $\ddot{q}_{d,i}$, angular velocity $\dot{q}_{d,i}$, and angular position $q_{d,i}$ of the wheel. The desired wheel torque $\tau_{d,i}$ is calculated using

$$\tau_{d,i} = J_{w,i}(\ddot{q}_{d,i} + K_{v,i}(\dot{q}_{d,i} - \dot{q}_i) + K_{p,i}(q_{d,i} - q_i)) + C_i(q_i, \dot{q}_i) + G_i(q_i), \quad (3)$$

where $J_{w,i}$ is the wheel inertia, $K_{v,i}$ and $K_{p,i}$ are the feedback gains, $C_i(q_i, \dot{q}_i)$ is the friction term seen at wheel i, and $G_i(q_i)$ is the gravity term seen at wheel i. In Fig. 5 $\overline{\tau}$ is the maximum torque of the drive motors and defines a saturation function that determines the torque τ_i actually commanded to the robot wheel. The coupling effects of the wheels are neglected due to the high gear ratio from the motor to the wheel.

IV. Electric Powered Wheelchair Control Based on Reference Model

Motivated by results in which a model reference control scheme was used with a walker [8], a motion control algorithm based on a reference model is used to address the interaction between the user and EPW. The resulting control architecture is shown in Fig. 6. User intentions,

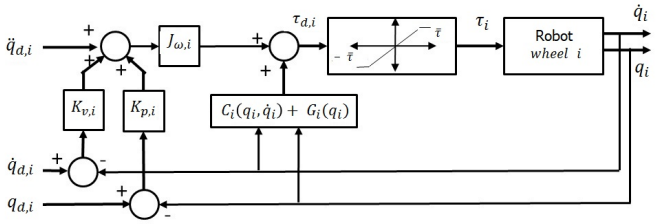

Fig. 5. This trajectory tracking controller (for robot wheel i) is used in both experimental platforms. It accepts desired wheel acceleration, velocity, and position. Additionally, it has gravity and friction compensation.

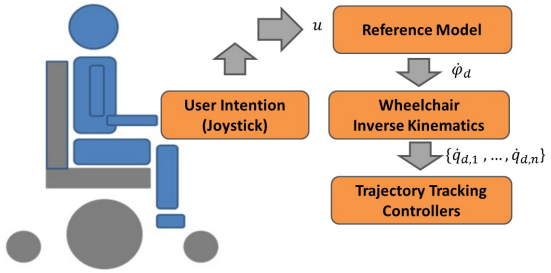

Fig. 6. EPW general control architecture using reference model and trajectory controller(low-level controller).

represented by the joystick displacements, are mapped into virtual force/torque values, which constitute the elements of $u \in \mathbb{R}^2$, the input to the reference model,

$$\mathbf{M_d}\ddot{\varphi}_d + \mathbf{D_d}\dot{\varphi}_d = u, \tag{4}$$

where

$$\mathbf{M_d} = \begin{bmatrix} m_x & 0 \\ 0 & m_\theta \end{bmatrix}, \ \mathbf{D_d} = \begin{bmatrix} d_x & 0 \\ 0 & d_\theta \end{bmatrix},$$
$$\dot{\varphi}_d = \begin{bmatrix} v_{R,d} \\ \omega_{R,d} \end{bmatrix}, \ u = \begin{bmatrix} u_x \\ u_\theta \end{bmatrix}, \tag{5}$$

and, referring to Fig. 7, the subscript x denotes relationship to the x_R-axis and subscript θ denotes rotation about the z_R-axis. The left wheel is denoted as wheel 1 and the right wheel as wheel 2. The output of the reference model is $\dot{\varphi}_d$ and the desired angular velocities $\{\dot{q}_{d,1}, \dot{q}_{d,2}\}$ for the 2 drive wheels are determined through the inverse kinematics. The desired accelerations $\{\ddot{q}_{d,1}, \ddot{q}_{d,2}\}$ and desired positions $\{q_{d,1}, q_{d,2}\}$ are then respectively determined by differentiation and integration of the desired velocities. The controller in Fig. 5 tracks $\ddot{q}_{d,i}$, $\dot{q}_{d,i}$, and $q_{d,i}$.

V. Slip Control Using Variable Reference Model and Maximum Tractive Force Estimate

Slip control along the longitudinal direction of an EPW can be accomplished through parameter variation in the reference model. The reference model in (4) with $u = [u_x \ 0]^T$ simplifies to

$$m_x\ddot{x}_R + d_x\dot{x}_R = u_x. \tag{6}$$

Assume that the vehicle is moving under driver control with nominal values of the parameters of the reference model (6) given by $m_x = m_{x,0}$ and $d_x = d_{x,0}$. The proposed slip control concept is based on monitoring the traction force

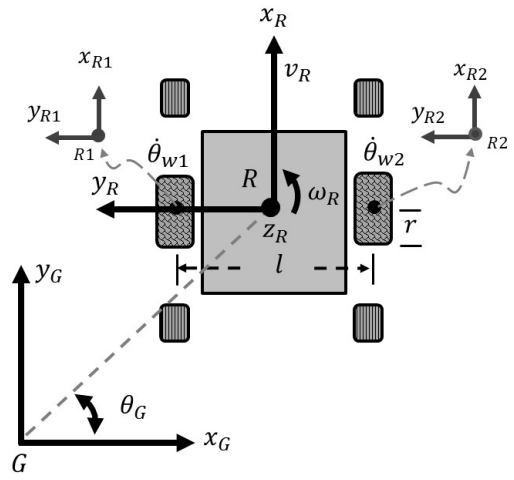

Fig. 7. This figure shows the kinematic diagram of the electric powered wheelchair

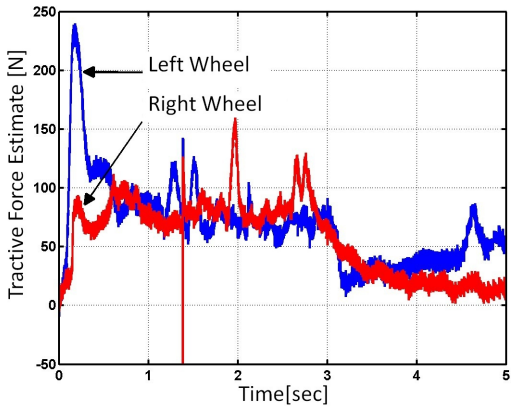

(a)

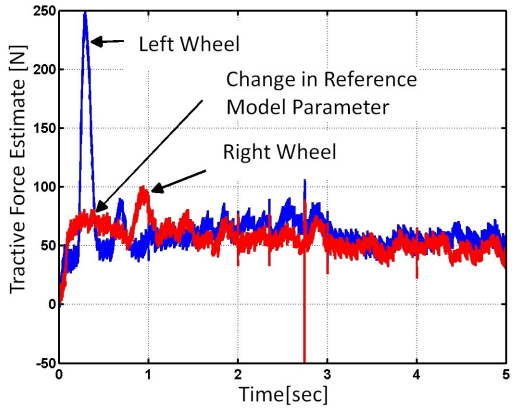

(b)

Fig. 8. (a) Under the baseline controller, as the right wheel slips, a significant difference between the left and right wheel tractive forces causes the EPW to curve to the right as shows in Fig. 10. (b) Using the slip mitigation control, the desired mass is changed and the tractive forces of both wheels are approximately equal, enabling the EPW to move straight as shown in Fig. 11.

estimate $\hat{F}_{d,i}$ for wheel i as computed in Fig. 3(b) as the vehicle accelerates over a given (small) period to determine an estimate $\hat{F}_{d,i_{max}}$ of the maximum tractive force for wheel i. We then define $\hat{F}_{d_{max}} = \min_{j\in\{1,2\}} \hat{F}_{d,j_{max}}$. Assume that the minimum occurs for wheel j_* and $\hat{F}_{d_{max}} = \hat{F}_{d,j_*}(t_*)$,

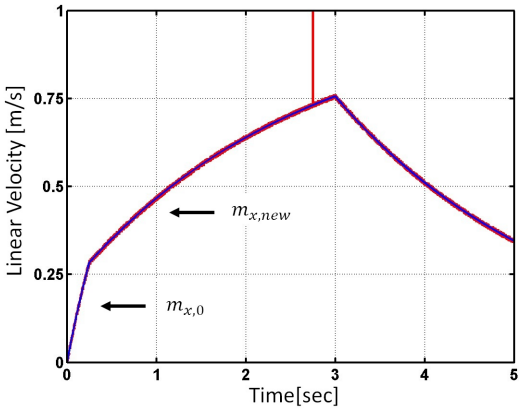

Fig. 9. Slip mitigation control applied to the EPW resulted in this linear velocity $\dot{x}_R$, which was measured using encoders. When m_x was updated to $m_{x,new} > m_{x,0}$ at $t = t_* = 0.29sec$, the acceleration slowed as expected.

the tractive force estimate for wheel j_* evaluated at time t_*. The idea is to modify (if necessary) m_x in (6) such that it produces future desired vehicle accelerations that do not require a tractive force from any of the wheels that exceeds $\hat{F}_{d_{max}}$. Note that since $\hat{F}_{d_{max}}$ is the minimum of the estimated maximum tractive force over each wheel, this strategy seeks to ensure that no wheel requires a tractive force not capable of being achieved by every other wheel. This is important since, for example, a vehicle can move longitudinally in a straight line only if the tractive force applied to each wheel is the same.

To determine a constraint on m_x, we first analyze wheel i to determine a constraint on $\ddot{x}_{R,i}$. The constraints on $\ddot{x}_{R,1}$ and $\ddot{x}_{R,2}$ are then mapped to a constraint on $\ddot{x}_R$ using the EPW's kinematics, which are based on Fig. 7. The translational dynamics (2) for wheel i are rewritten here as

$$M_i \ddot{x}_{R,i} = F_{d,i} - F_{r,i}. \tag{7}$$

It follows from (7) that if we want to ensure $F_{d,i} < \hat{F}_{d_{max}}$, then if $F_{r,i} << F_{d,i}$, it is desired that

$$\ddot{x}_{R,i} < \hat{F}_{d_{max}}/M_i. \tag{8}$$

Given that $[\ddot{x}_R \;\; \ddot{\theta}_R]^T = \mathbb{J}[\ddot{x}_{R,1}, \ddot{x}_{R,2}]^T$, where $\mathbb{J}$ is the wheelchair's Jacobian matrix. It is also desired that

$$\ddot{x}_R < \hat{F}_{d_{max}} \sum_{i=1}^{2} \frac{\mathbb{J}_{1,i}}{M_i}, \tag{9}$$

where $\mathbb{J}_{1,i}$ is the $(1,i)$ element of $\mathbb{J}$. For the wheelchair of Fig. 4, which has the kinematics of Fig. 7, $\mathbb{J}_{1,1} = \mathbb{J}_{1,2} = 1/2$ and $M_1 = M_2 = M/2$, where $M = 90kg$ is the total mass of the wheelchair. To ensure (9) is satisfied use (6) to choose

$$m_x > \frac{1}{\hat{F}_{d_{max}} \sum_{i=1}^{2} \frac{\mathbb{J}_{1,i}}{M_i}} \left(u_x(t_*) - d_{x,0} \dot{x}_R(t_*) \right). \tag{10}$$

The inequality in (10) essentially ensures that if the initial command profile $u_x(t)$ were repeated, the traction force required by any of the wheels will not exceed $\hat{F}_{d_{max}}$. Note that if $m_x = m_{x,0}$ satisfies (10), then m_x does not have to be increased. Also, once m_x is increased, it can later be reduced, for example, when the acceleration of the EPW is smaller than some threshold.

VI. Experiments and Results

Experiments were performed to evaluate the slip mitigation approach for an EPW. These experiments did not involve a human driver. Instead the wheelchair was commanded remotely as if a user were choosing the joystick setting to command the wheelchair to move straight in the longitudinal direction, i.e., $u_\theta = 0$. In all the experiments, the input u_x was given by

$$u_x = \begin{cases} 100\text{N}, & t \in [0,3] sec \\ 0, & t > 3sec. \end{cases} \tag{11}$$

Initially $m_x = m_{x,0} = 75kg$ and $d_x = d_{x,0} = 100kg/s$. These values were chosen so that the reference model (6) yields a maximum commanded acceleration $\ddot{x}_{R,d}$ from rest of $1.33m/s^2$ and a maximum steady-state velocity $\dot{x}_{R,d}$ of $1m/s$. The actual maximum linear acceleration for the experimental setup shown in Fig. 4 is $2m/s^2$ and the maximum linear velocity is $1.5m/s$, while the actual mass of the wheelchair is $90kg$. Referring to Fig. 3, the gear resistances $\tau_{r,1}$ and $\tau_{r,2}$ were determined by measuring the torque of each wheel while the EPW was raised so that the wheels were not in contact with the ground.

Experiments were conducted to evaluate the EPW movements. The first set of experiments used the reference model (6) for both wheels with $m_x = m_{x,0}$ and $d_x = d_{x,0}$, which is the baseline control. The second set allowed the value of m_x to change to satisfy (10), such that slip mitigation control was enabled. As shown in Fig. 10 the right wheels of the EPW were initially placed on a slippery surface, which was an aluminum sheet covered with soapy water, and the left wheels were placed on a high traction surface, which was a vinyl floor. Since the vehicle is commanded to move straight in the longitudinal direction, the tractive forces applied to the 2 wheels should be approximately equal, so that it is desired that $\hat{F}_{d,1} = \hat{F}_{d,2}$.

Fig. 10 (a)-(d) show snapshots of the EPW trajectory under baseline control. Notice that the EPW curves to the right due to the loss of traction in the right drive wheel. Fig. 8(a) shows the estimated driving forces $\hat{F}_{d,1}$ and $\hat{F}_{d,2}$. Note that in general $\hat{F}_{d,1} \neq \hat{F}_{d,2}$, which accounts for the lack of linear motion.

In the implementation of slip control, the value of $\hat{F}_{d,i}$ was continuously updated during acceleration and if $\hat{F}_{d,i} > \hat{F}_{d,i_{max}}$ then $\hat{F}_{d,i_{max}} \leftarrow \hat{F}_{d,i}$. The detection of $\hat{F}_{d,i_{max}}$ stopped if $(\hat{F}_{d,i_{max}} - \hat{F}_{d,i}) > 3\sigma$, where $\sigma = 7.5N$, is the standard deviation of $\hat{F}_{d,i}(t)$ for $t \in [t_0, t_0 + 5sec]$, an interval at time in which the vehicle is moving only on the high traction vinly surface. Using this method $\hat{F}_{d_{max}} = \hat{F}_{d,2}(0.25sec)$. Due to the right wheel's movement on the slippery surface, it was found at time $t = t_* = 0.29sec.$ that (10) was violated. The mass was then updated using

$$m_x = m_{x,0} + \beta \frac{M_{i_*}}{\hat{F}_{d_{max}}} \left(u_x(t_*) - d_{x,0} \dot{x}_R(t_*) \right), \tag{12}$$

(a) (b) (c) (d)

Fig. 10. Snapshots of the wheelchair with the command in (11). The right wheel is on a slippery ground and the wheelchair is controlled without the proposed slip reduction approach.

(a) (b) (c) (d)

Fig. 11. Snapshots of the wheelchair with the command in (11). The right wheel is on a slippery ground and the wheelchair is controlled with the proposed slip reduction approach.

where β is a tuning factor that helps to account for the overestimation of $\hat{F}_{d_{max}}$. In these experiments $\beta = 1$ and m_x was updated to relatively $m_{x,new} = 255kg$. Fig. 11 (a)-(d) shows that the EPW behavior was able to move straight (with only a small heading error) due to the slip mitigation control, although the right drive wheel of the EPW did experience some initial slip as evidenced by the fact that Fig. 8 (b) shows that before m_x was updated at $t = t_* = 0.29sec.$, $\hat{F}_{d,2}$ was substantially less than $\hat{F}_{d,1}$ due to the loss of traction in wheel 2 as it moved on the slippery surface. However, after the update of m_x, $\hat{F}_{d,1} \approx \hat{F}_{d,2}$ as desired, resulting in the desired linear motion. The slip control evaluation was repeated five times and the average heading error was approximately 3.82°.

VII. Conclusion

This study presented an approach to slip mitigation control for an EPW based on variable mass-damper reference model. An estimate of the maximum tractive force for each wheel is determined and the minimum of the maximum tractive forces is used to solve for the feasible linear accelerations of the wheels. The vehicle Jacobian matrix is used to transform the constraints on the wheel accelerations to a constraint on the acceleration of the wheelchair body, which in turn yields a constraint on the mass of the reference model. When the mass constraint is violated, i.e., slip occurs, the mass is updated to ensure that future trajectories do not require any wheel to have more tractive force that can be provided to each of the wheels. An experiment was performed to show the viability of this approach. Although the developments are only for movement in the longitudinal direction the analysis is based on the wheels and can be extended to general curvilinear motion.

Future work will focus on extensions and experiments for general EPW motion. Additionally, other exterioceptive sensors such as an inertial measurement unit will be considered to improve the accuracy of the estimation of the tractive forces.

References

[1] K. Choi, M. Sato, and Y. Koike. A new, human-centered wheelchair system controlled by the EMG signal. In *2006 International Joint Conference on Neural Networks*, pages 4664–4671, 2006.

[2] D. Ding and R. Cooper. Electric powered wheelchairs: A revuew of current technology and insight into future directions. *IEEE Control Systems Magazine*, pages 22–34, 2005.

[3] K. Fujii and H. Fujimoto. Traction control based on slip ratio estimation without detecting vehicle speed for electric vehicle. In *Power Conversion Conference*, pages 688–693, 2007.

[4] F. Gustafsson. Slip-based tire-road friction estimation. *Automatica*, 33(6):1087–1099, 1997.

[5] Y. Hori, Y. Toyoda, and Y. Tsuruoka. Traction control of electric vehicle: Basic experimental results using the test ev "UOT Electric March". *IEEE Transactions on Industry Applications*, 34(5):1131–1138, 1998.

[6] Y. Hori, Y. Toyoda, and Y. Tsuruoka. Future vehicle driven by electricity and control research on four-wheel-motored "UOT Electric March II". *IEEE Transactions on Industrial Electronics*, 51(5):954–962, 2004.

[7] O. Chuy Jr., Y. Hirata, and K. Kosuge. A new control approach for a robotic walking support system in adapting user characteristic. *IEEE Trans. Syst., Man, Cybern. C*, 36(6):725–733, 2006.

[8] O. Chuy Jr., Y. Hirata, Z. Wang, and K. Kosuge. A control approach based on passive behavior to enhance user interaction. *IEEE Transactions on Robotics*, 23(5):899–908, October 2007.

[9] H. Kataoka, H. Sado, I. Sakai, and Y. Hori. Optimal slip ratio estimator for traction control system of electric vehicle based on fuzzy inference. *Elect. Eng. Jpn.*, 135:5663, 2001.

[10] H. Sado, S. Sakai, and Y. Hori. Road condition estimation for traction control in electric vehicle. In *Proceedings of the IEEE International Symposium on Industrial Electronics*, pages 973 – 978, 1999.

[11] B. Subudhi and S. Ge. Sliding-mode-observer-based adaptive slip ratio control for electric and hybrid vehicles. *IEEE Transactions on Intelligent Transportation Systems*, 13(4):1617–1626, 2012.

[12] G. Vasiljevic, K. Griparic, and S. Bogdan. Slip-based traction control system with an on-line road condition estimation for electric vehicles. In *2012 IEEE International Conference on Control Applications*, pages 395–400, 2012.

[13] H. Wang, B. Salatin, G. Grindle, D. Ding, and R. Cooper. Real-time model-based electrical powered wheelchair control. In *Medical Engineering Physics*, pages 1244–1254, 2009.

[14] D. Yin and Y. Hori. A novel traction control for electric vehicle without chassis velocity. *INTECH ISBN 978-953-7619-55-8*, pages 121–140, 2010.

[15] D. Yin, S. Oh, and Y. Hori. A novel traction control for ev based on maximum transmissible torque estimation. *IEEE Transactions on Industrial Electronics*, 56(6):2086–2094, 2009.

[16] H. Yu, M. Spenko, and S. Dubowsky. An adaptive control system for an intelligent mobility aid for the elderly. *Auton. Robots*, 15:53–66, 2003.